INTERNATIONAL JOURNAL OF PRECISION ENGINEERING AND MANUFACTURING Vol. 18, No. 3, pp. 375-380 MARCH 2017 / 375

REGULAR PAPER

DOI: 10.1007/s12541-017-0045-0
ISSN 2234-7593 (Print) / 2005-4602 (Online)

Hysteresis Curve Analysis of a Cycloid Reducer Using Non-Linear Spring with a Dead Zone

Anh Duc Pham[1], The Linh Tran[2], and Hyeong-Joon Ahn[3,#]

1 Department of Software Convergence, Graduate School, Soongsil University, 369 Sangdo-ro, Dongjak-gu, Seoul, 34056, South Korea
2 Department of Mechanical Engineering, Graduate School, Soongsil University, 369 Sangdo-ro, Dongjak-gu, Seoul, 34056, South Korea
3 Department of Mechanical Engineering, Soongsil University, 369 Sangdo-ro, Dongjak-gu, Seoul, 34056, South Korea
Corresponding Author / E-mail: ahj123@ssu.ac.kr, TEL: +82-2-820-0654,FAX: +82-2-820-0668

KEYWORDS: Cycloid reducer, Hysteresis curve, FE analysis, Nonlinear spring with dead zone

Cycloid reducers are widely used for high-precision industrial instruments and robots because of many advantages: high efficiency, high stiffness and a high reduction ratio in a compact size. Nevertheless, the few studies that have investigated the hysteresis characteristics of a cycloid reducer used a time-consuming iterative procedure. This paper presents an efficient FE analysis procedure for the hysteresis characteristics of a cycloid reducer using a nonlinear spring with a dead zone. First, we introduced a cycloid reducer and performed a kinematic analysis of the cycloid disk with tolerance. Next, connecting elements of the cycloid reducer such as the input bearing, pin-roller and output roller were approximated as nonlinear springs with a dead zone. In particular, the dead zone for the nonlinear springs was introduced to represent the clearance of each connecting element. Then, a full FE model of the cycloid reducer was built incorporating the nonlinear springs, and the hysteresis characteristic of the cycloid reducer was directly evaluated at one time so as to significantly save its analysis effort and time. Results showed that tolerance had a great effect on torque and the torsional angle relationship of the cycloid reducer. such as lost motion, back lash and torsional rigidity.

Manuscript received: September 27, 2016 / Revised: October 22, 2016 / Accepted: October 27, 2016

1. Introduction

From its first appearance in the 1960s, industrial robots have played important roles in improving both manufacturing quality and productivity. With the improvement of technical supports, industrial robots are performing many different roles as picking, packing, testing or assembling in modern industrial chains. As a report by the International Federation of Robotics (IFR) shows, the stock of industrial robots is reaching 1 million units globally.[1]

Recently, low-cost table-top robots have gained attention as potential candidates for industrial automatic manufacturing chains and are expected to replace human laborers at a lower price in the near future. Although some low-cost robotic arms have advanced safety features as well as easy deployment,[2] the performance of low-cost robots is still governed by conventional mechanical system requirements such as dynamic performance, torque or load capacity and accuracy.

High precision reducers such as cycloid reducers and harmonic drives have been adopted to meet the mechanical system requirements of industrial robots. Interestingly, the performance of these reducers governs the overall robot performance.[3,4] The performance of reducers can be estimated with a hysteresis curve, rotational transmission error and efficiency.[5]

Hysteresis curve is an integrated characteristic of two important performances: torsional stiffness and backlash. A procedure of measuring a hysteresis curve is as follows: when torque is applied to the output shaft while the input shaft is fixed, the output shaft has a small rotational motion, according to the torque applied. However, the torque-output rotation characteristics are not the same for loading and unloading, which is called the hysteresis curve in Fig. 1. Many important characteristics such as torsional rigidity, lost motion and backlash are defined from the hysteresis curve.[3]

There was previous research on the hysteresis characteristics of high precision reducers. In a harmonic drive, torsional rigidity was first studied by mathematical methods,[6-8] FEM[9] and experiments.[10] In addition, the torsional rigidity of a two-stage cycloid drive without tolerance was analyzed by an iteration FE analysis and Hertz theory.[11] Moreover, the lost motion of a cycloid reducer was analyzed with the iterative procedure of kinematic and FE analyses.[3] However, these iterative analyses are not only time-consuming, but also complicate procedures.

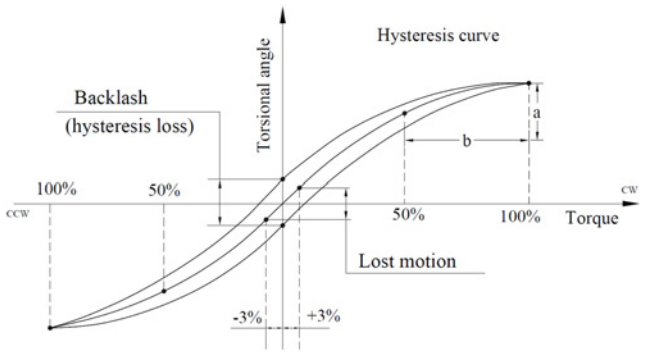

Fig. 1 Hysteresis curve of a precision reducer[3]

This paper presents an efficient FE analysis of hysteresis characteristic of a cycloid reducer using a nonlinear spring with a dead zone. First, we introduced a cycloid reducer and performed a kinematic analysis of the cycloid reducer considering tolerance. Next, connecting elements of the cycloid reducer such as the input bearing, pin-roller and output roller were approximated as nonlinear springs with a dead zone. In particular, the dead zone for nonlinear spring was introduced to incorporate clearance of the connecting element. Then, a full FE model of the cycloid reducer was built and the hysteresis characteristics of the cycloid reducer were directly analyzed at one time. Lost motion, back lash and torsional rigidity were evaluated from the hysteresis characteristic of the cycloid reducer.

2. Cycloid Reducer with Clearances

2.1 Principle

A one-stage cycloid reducer comprises many components, as shown in Fig. 2. The main elements are an input eccentric shaft, a cycloid disk engaged with pin-rollers, and an output mechanism. In principle, wobble motion is transferred from the input by the eccentric shaft through a bearing to the cycloid disk. The wobble motion is converted into a pure rotating motion with the output mechanism consisting of output rollers and a sliding plate.

2.2 Clearances of cycloid reducers

Clearances are necessary for a cycloid reducer to tolerate thermal expansion, manufacturing errors, as well as assembling its components. Although a cycloid disk without any clearance has contact with half of the pin-rollers, clearances in a cycloid reducer affect the amount of contact as well as hysteresis curve or the torque-output rotation relationship.

In this study, clearances at the two main connection elements, such as the cycloid disk and the output mechanism, are considered, as shown in Fig. 3. Since each connecting element has not only clearance but also stiffness, the hysteresis characteristic of the cycloid reducer should be investigated with consideration of both clearance and the stiffness of the connection elements. Only nonlinear stiffness is considered exceptionally for the input bearing, since it has a very small clearance and a small effect on the output torsion angle.

The tolerance of the cycloid disk affects each contact with the pin-rollers differently. According to the given parameters of a cycloid reducer in Table 1, clearances between the cycloid disk and the pin-rollers are calculated and shown in Fig. 4. This simple kinematic analysis shows that uniform tolerances of the pin-rollers do not render uniform clearances at the contact points.[3,12-15]

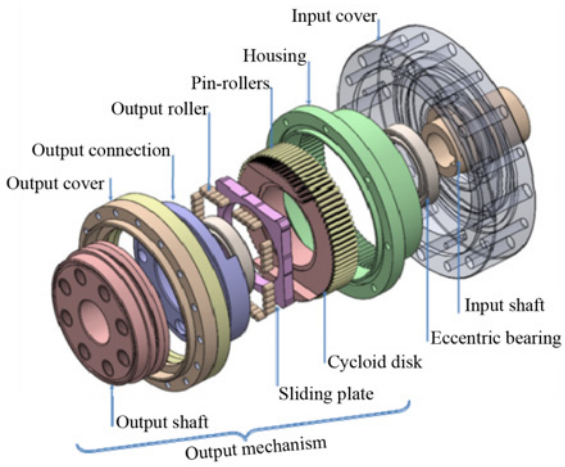

Fig. 2 Cycloid reducer

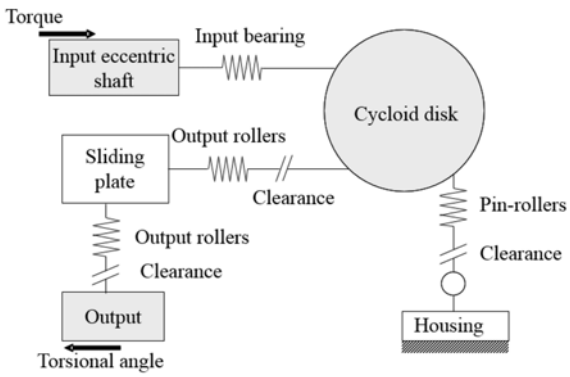

Fig. 3 Torque transfer path of the cycloid reducer

Table 1 Specification of the cycloid reducer

Parameter	Value
Eccentricity (mm)	0.35
Radius of housing (mm)	32.5
Outer diameter of housing (mm)	69
Radius of pin-roller (mm)	0.8
Number of pin-roller	80
Number of output roller	40
Reduction ratio	79
Radius of output roller (mm)	1.5

2.3 Nonlinear contact spring with a dead zone

A nonlinear spring with a dead zone was introduced to model the connecting elements that have both nonlinear stiffness and clearance. Bearings or rollers on the cycloid disk or the output mechanism can be modelled as nonlinear spring considering the Hertz contact theory. In addition, a dead zone was added to the nonlinear spring with

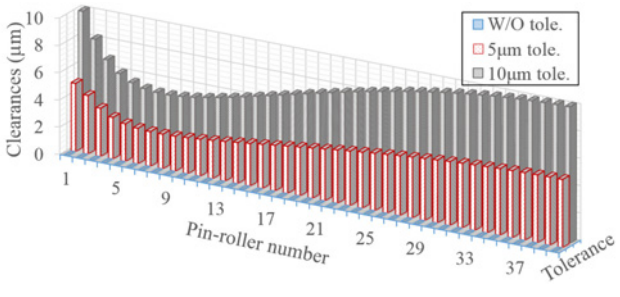

Fig. 4 Clearances between the pin-rollers and the cycloid disk with various tolerances

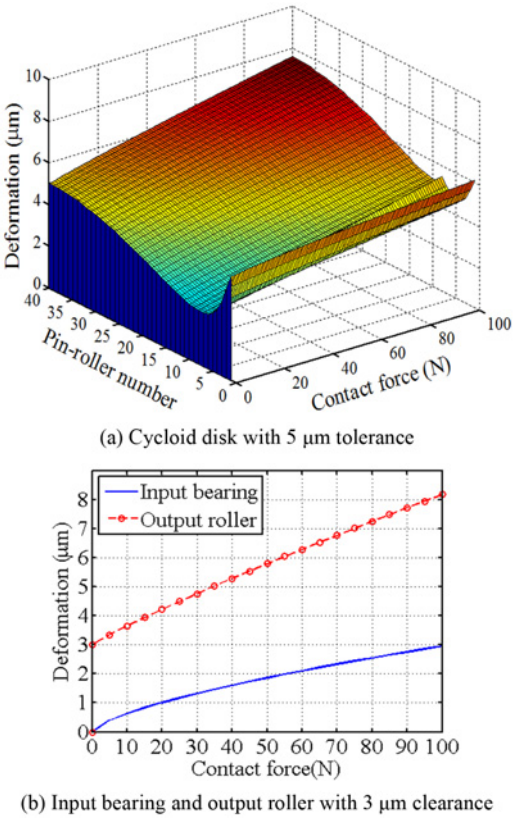

Fig. 5 Non-linear contact stiffness of the connecting elements

consideration for clearance.

Contacts between the cycloid disk and pin-rollers can be approximated as Hertz contacts between two cylindrical bodies. According to Hertz contact theory, contact stiffness (or contact force per unit depth) can be expressed as a non-linear function of the contact forces, the material properties and the geometries of the two contact cylinders. Therefore, contact stiffness at each contact point varies according to the curvature at contact point of the cycloid disk, as shown in Fig. 5(a). In addition, a dead zone is added to the nonlinear contact stiffness incorporating the kinematic analysis.

The contact stiffness of the input bearing and the output roller is shown in Fig. 5(b). Bearing stiffness can similarly be calculated based on Hertz contact theory.[16-19] In addition, contact between the output roller and the sliding plate can be approximated as Hertz contact of a

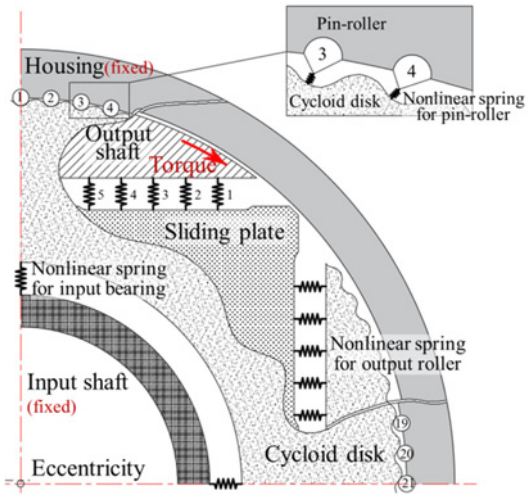

Fig. 6 Schematic diagram of the FE model of the cycloid reducer

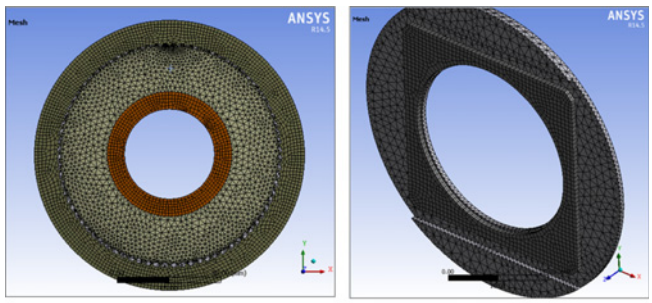

Fig. 7 FE model of the cycloid reducer

cylinder on a flat surface, too. Furthermore, the dead zone is inserted to the nonlinear spring to model the clearance of the output roller.

3. Hysteresis Curve Analysis

3.1 FE model

A schematic diagram of a FE model for the cycloid reducer is shown in Fig. 6. First, the FE model had 1 mm thickness to reduce both the number of elements and the computation time. Second, all connecting elements such the input bearing, pin-rollers and output rollers were modeled as nonlinear springs with a dead zone. The cycloid disk had a planar motion, while both the sliding plate and output shaft had only a rotary motion. In addition, the housing and the input shaft were fixed. In case of contact between the cycloid disk and pin-rollers, sharp pointing triangular structures were built from the housing to theoretical contact points of the cycloid disk, and small uniform gaps (50 μm) at the contact points were introduced to insert the nonlinear springs.

A generated mesh for the FE model in ANSYS Workbench is shown in Fig. 7. Triangular meshes of 1.5 mm were generated, and fine spheres and mapped meshes of half size were introduced for the contact region. The total number of elements and nodes were respectively 28,996 and 74,139.

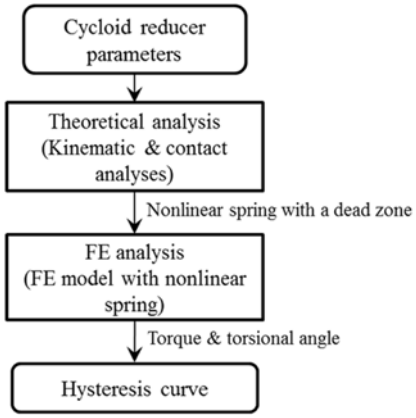

Fig. 8 Procedure for hysteresis analysis of the cycloid reducer

3.2 Hysteresis analysis procedure

In order to efficiently analyze the torque-torsion angle relationship without any iteration between theoretical and FE analyses, a sequential procedure of kinematic and FE analyses is shown in Fig. 8. First, a kinematic analysis of the cycloid disk with tolerance determined its clearance to the pin-rollers. At the same time, the nonlinear stiffness of each connecting element such as input bearing, pin-rollers and output rollers was calculated based on Hertz contact theory. A nonlinear spring with a dead zone was generated considering the clearance and the nonlinear stiffness. Then, an FE analysis of the cycloid reducer was performed to calculate the contact force and deformation of the connecting elements. Finally, the hysteresis curve was evaluated from the torque and torsional angle of the output shaft without any iteration.

4. Analysis Results

4.1 Contact force and deformation

In cases of 5 and 10 μm uniform tolerances of the cycloid disk, clearance and deformation of the springs at contact points under 0.36 Nm (3% of rated torque) are shown in Fig. 9. The pin-roller was numbered clockwise, as shown in Fig. 6. If the clearance at a contact point was larger than the spring deformation, the nonlinear spring was still in the dead zone and the pin-roller lost contact with the cycloid disk. Therefore, 5 pin-rollers had contacts with the cycloid disk of 5 mm tolerance while 4 pin-rollers had contacts with the cycloid disk of 10 mm tolerance. In addition, contact deformation could be calculated by subtracting clearance from the nonlinear spring deformation.

As the output torque and the tolerance increased, contact forces and deformations of pin-rollers were calculated and shown in Figs. 10 and 11. The number of contacts and the contact force distribution of the cycloid disk changed due to both bearing stiffness and disk tolerance, as shown in Fig. 10(a) and (b). In addition, peak contact force and the number of contacts increased as the output torque increased, as shown in Fig. 11(a) and (b).

Deflection of the input bearing with various tolerances of both the cycloid disk and the output rollers were calculated and shown in Fig. 12. As the output torque increased, the bearing was deflected more and the cycloid disk moved to the right. Moreover, the bearing was

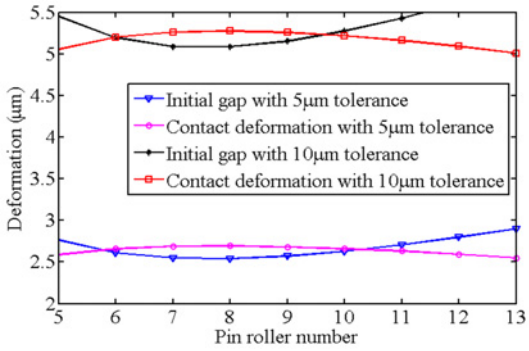

Fig. 9 Clearance and spring deformation at contact points of the cycloid reducer under 0.36 Nm of torque

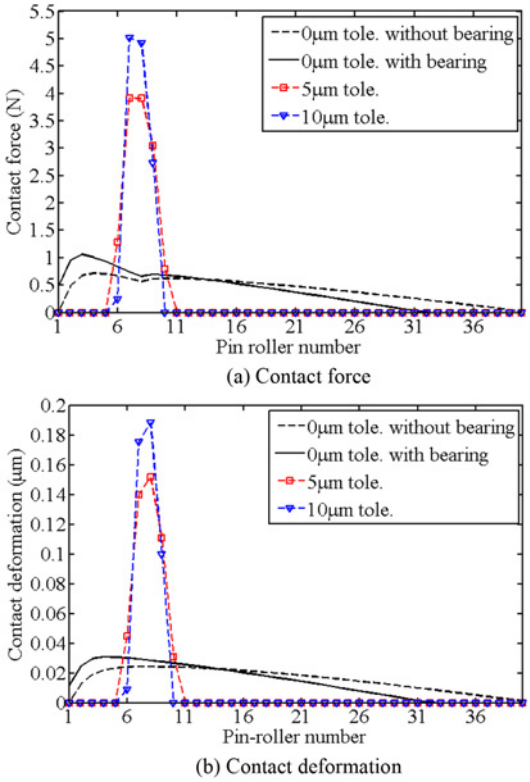

Fig. 10 Contact force and contact deformation at 0.36 Nm of torque

deflected and fluctuated more as the tolerances of the cycloid disk and the output rollers increased. Here, D and R in Fig. 12 denote the cycloid disk and output roller, respectively.

Contact forces and deformations of output rollers with various tolerances are shown in Fig. 13. Output rollers are numbered from outside to inside, as shown in Fig. 6. As the clearance increased, contact force was concentrated to the outside output roller.

4.2 Hysteresis curve

From the procedure in Fig. 8, the torque and torsional angle relationship of the cycloid reducer with various tolerances is shown in Fig. 14. Proposed analysis method allows that backlash, lost motion and torsional rigidity of the cycloid reducers, with and without

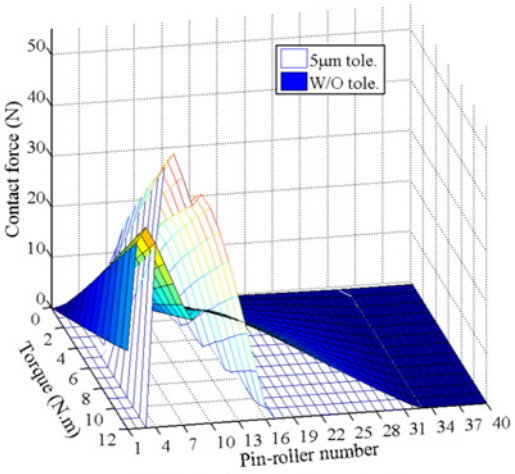

(a) Contact force with various torque

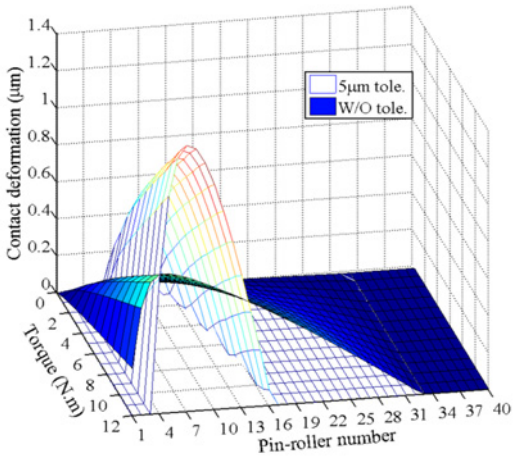

(b) Contact deformation with various torque

Fig. 11 Contact force and contact deformation between cycloid disk and pin roller under increasing torque

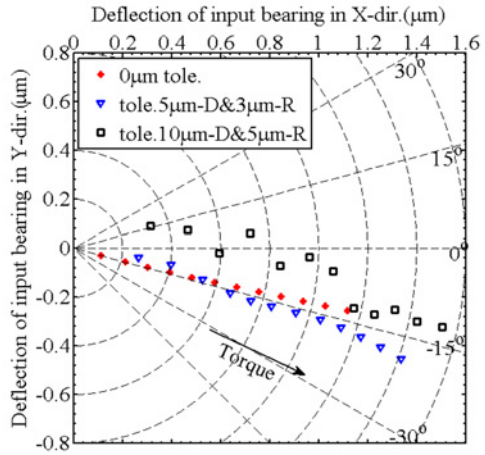

Fig. 12 Deflection of the input bearing with various tolerances in the cycloid disk and the output roller

tolerance, are evaluated at once, as shown in Table 2. The backlash and the lost motion had similar values as the tolerance increased. However, the lost motion had a bigger value than the backlash, due to the

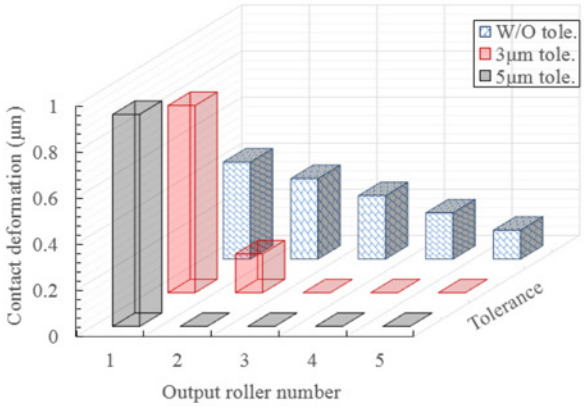

(a) Contact deformation with various tolerance

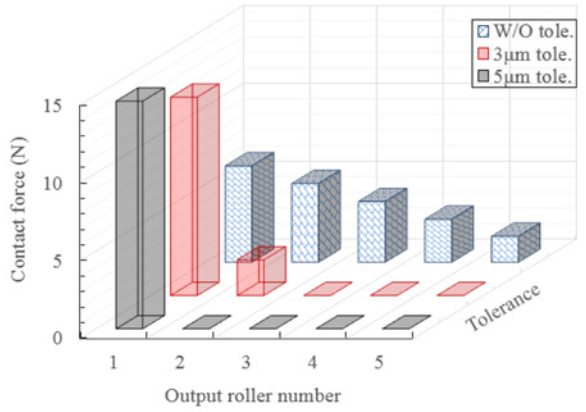

(b) Contact force with various tolerance

Fig. 13 Contact force of output roller with various clearance at 0.36 Nm of torque

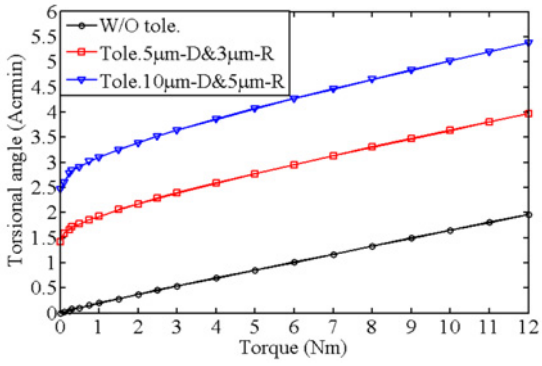

Fig. 14 Torque and torsional angle relationship of the cycloid reducer with various tolerances

Table 2 Comparison of backlash and lost motion of cycloid reducer

Tolerance	0 μm	Tole. 5 μm-D & 3 μm-R*	Tole. 10 μm-D & 5 μm-R
Backlash (acrmin)	0	1.419	2.470
Lost motion (arcmin)	0.153	1.714	2.842
Torsional rigidity (Nm/acrmin)	6.337	5.897	5.401

*D and R denote the cycloid disk and output roller, respectively.

stiffness of connection elements in the cycloid reducer. In addition, the torsional stiffness decreased as the tolerance increased.

5. Conclusion

This paper presents an efficient FE analysis of hysteresis characteristics of a cycloid reducer using a non-linear spring with a dead zone. Connecting elements of the cycloid reducer, such as the input bearing, the pin-rollers and the output rollers were approximated as nonlinear springs with a dead zone. A full FE model of the cycloid reducer was built and the hysteresis characteristics of the cycloid reducer were directly evaluated at one time so as to significantly reduce its analysis effort and time. Tolerance had a great effect on the torque and torsional angle relationship of the cycloid reducer, such as lost motion, back lash and torsional rigidity.

REFERENCES

1. Wallén, J., "The History of the Industrial Robot," Linköping University Electronic Press, 2008.
2. Universal Robots, "UR5 Robot," https://www.universal-robots.com/products/ur5-robot/ (Accessed 2 FEB 2017)
3. Tran, T. L., Pham, A. D., and Ahn, H.-J., "Lost Motion Analysis of One Stage Cycloid Reducer Considering Tolerances," Int. J. Precis. Eng. Manuf., Vol. 17, No. 8, pp. 1009-1016, 2016.
4. Machine Design, "Improve the Productivity of Your Factory Automation Systems with Lightweight Gears and Actuators," http://machinedesign.com/motion-control/improve-productivity-your-factory-automation-systems-lightweight-gears-and-actuators (Accessed 2 FEB 2017)
5. Nabtesco, "Precision Reduction Gear RV: E Series / C Series / Original Series," www.nabtescomotioncontrol.com/pdfs/rv-e-c-series.pdf (Accessed 2 FEB 2017)
6. Taghirad, H. D. and Belanger, P. R., "Modeling and Parameter Identification of Harmonic Drive Systems," Transactions-American Society of Mechanical Engineers Journal of Dynamic Systems Measurement and Control, Vol. 120, No. 4, pp. 439-444, 1998.
7. Tjahjowidodo, T., Al-Bender, F., and Van Brussel, H., "Theoretical Modelling and Experimental Identification of Nonlinear Torsional Behaviour in Harmonic Drives," Mechatronics, Vol. 23, No. 5, pp. 497-504, 2013.
8. Dhaouadi, R., Ghorbel, F. H., and Gandhi, P. S., "A New Dynamic Model of Hysteresis in Harmonic Drives," IEEE Transactions on Industrial Electronics, Vol. 50, No. 6, pp. 1165-1171, 2003.
9. Rhéaume, F. E., Champliaud, H., and Liu, Z., "Understanding and Modelling the Torsional Stiffness of Harmonic Drives through Finite-Element Method," Proceedings of the Institution of Mechanical Engineers, Part C: Journal of Mechanical Engineering Science, Vol. 223, No. 2, pp. 515-524, 2009.
10. Kircanski, N. M. and Goldenberg, A. A., "An Experimental Study of Nonlinear Stiffness, Hysteresis, and Friction Effects in Robot Joints with Harmonic Drives and Torque Sensors," The International Journal of Robotics Research, Vol. 16, No. 2, pp. 214-239, 1997.
11. Kim, K.-H., Lee, C.-S., and Ahn, H.-J., "Torsional Rigidity of a Cycloid Drive Considering Finite Bearing and Hertz Contact Stiffness," Proc. of ASME International Design Engineering Technical Conferences and Computers and Information in Engineering Conference, pp. 125-130, 2009.
12. Blanche, J. G. and Yang, D. C. H., "Cycloid Drives with Machining Tolerances," ASME Journal of Mechanisms, Transmissions, Vol. 111, No. 3, pp. 337-344, 1989.
13. Yang, D. C. H. and Blanche, J. G., "Design and Application Guidelines for Cycloid Drives with Machining Tolerances," Mechanism and Machine Theory, Vol. 25, No. 5, pp. 487-501, 1990.
14. Fang, S., Liu, Y., Wang, H., Taguchi, T., and Takeda, R., "Research on the Compensation Method for the Measurement Error of Cycloidal Gear Tooth Flank," Int. J. Precis. Eng. Manuf., Vol. 15, No. 10, pp. 2065-2069, 2014.
15. Kim, J.-G., Park, Y.-J., Lee, G.-H., and Kim, J.-H., "An Experimental Study on the Effect of Carrier Pinhole Position Errors on Planet Gear Load Sharing," Int. J. Precis. Eng. Manuf., Vol. 17, No. 10, pp. 1305-1312, 2016.
16. Park, Y.-J., Kim, J.-G., Lee, G.-H., Kim, Y.-J., and Oh, J.-Y., "Effects of Bearing Characteristics on Load Distribution and Sharing of Pitch Reducer for Wind Turbine," Int. J. Precis. Eng. Manuf.-Green Tech., Vol. 3, No. 1, pp. 55-65, 2016.
17. Johnson, K. L., "Contact Mechanics," Cambridge University Press, pp. 84-106, 2001.
18. Hamrock, B. J. and Anderson, W. J., "Rolling-Element Bearings," NASA Technical Reports Server, Report No. NASA-RP-1105, 1983.
19. New Hampshire Ball Bearings, Inc., "Roller and Ball Bearings Design Guide," 2010. https://www.universal-robots.com/products/ur5-robot/ (Accessed 2 FEB 2017)